Revista Virtual de Química
ISSN 1984-6835

Artigo

Drug-Protein Interaction: Spectroscopic and Theoretical Analysis on the Association between HSA and 1,4-Naphthoquinone Derivatives

Ferreira, R. C.;* Chaves, O. A.; de Oliveira, C. H. C. S.; Ferreira, S. B.; Ferreira, V. F.; Sant'Anna, C. M. R.; Cesarin-Sobrinho, D.; Netto-Ferreira, J. C.

Rev. Virtual Quim., **2018**, *10* (2), 432-447. Data de publicação na Web: 5 de abril de 2018

http://rvq.sbq.org.br

Interação Proteína-Fármaco: Análises Espectroscópica e Teórica sobre a Associação entre ASH e Derivados de 1,4-Naftoquinona

Resumo: A interação entre albumina sérica humana (ASH) e dois derivados biologicamente ativos de 1,4-naftoquinona (**FNP** e **FNP4Br**) foi estudada por dicroísmo circular, fluorescência estacionária e fluorescência resolvida no tempo sob condições biológicas a 305 K, 310 K e 315 K. Para oferecer uma explicação a nível molecular, foram realizados cálculos de ancoramento molecular. Uma associação no estado estacionário entre a albumina e as amostras foi observada por estudos espectroscópicos. A ligação é espontânea, moderada, pode perturbar a estrutura secundária da albumina e aumentar a hidrofobicidade ao redor do resíduo Trp-214, isso provavelmente devido a efeitos hidrofóbicos. Parâmetros termodinâmicos e ancoramento molecular sugerem ligação de hidrogênio e interações eletrostáticas (dipolo-dipolo) como as principais forças para a associação ASH:**FNP** e ASH:**FNP4Br**.

Palavras-chave: Albumina sérica humana; Derivados de 1,4-naftoquinona; Espectroscopia; Ancoramento molecular.

Abstract

The interaction between human serum albumin (HSA) and two biologically active 1,4-naphthoquinone derivatives (**FNP** and **FNP4Br**) was studied by circular dichroism, steady-state and time-resolved fluorescence under biological conditions at 305 K, 310 K and 315 K. In order to offer a molecular level explanation, molecular docking calculations were carried out. A ground state association between albumin and the samples was observed by spectroscopic studies. The binding is spontaneous, moderate, can perturb the secondary structure of the albumin and increase the hydrophobicity around the Trp-214 residue, probably due the hydrophobic effect. Thermodynamic parameters and molecular docking results suggest hydrogen bonding and electrostatic interactions (dipole-dipole) as the main binding forces for the association HSA:**FNP** and HSA:**FNP4Br**.

Keywords: Human serum albumin; 1,4-Naphthoquinone derivatives; Spectroscopy; Molecular docking.

* Universidade Federal Rural do Rio de Janeiro, Departamento de Química, CEP 23890-000, Seropédica-RJ, Brazil.
romulorcf@yahoo.com.br
DOI: 10.21577/1984-6835.20180032

Volume 10, Número 2 Março-Abril 2018

Revista Virtual de Química
ISSN 1984-6835

Drug–Protein Interaction: Spectroscopic and Theoretical Analysis on the Association between HSA and 1,4-Naphthoquinone Derivatives

Romulo C. Ferreira,[a,*] Otávio Augusto Chaves,[a] Cosme H. C. dos S. de Oliveira,[a] Sabrina B. Ferreira,[b] Vitor F. Ferreira,[c] Carlos Mauricio R. Sant'Anna,[a] Dari Cesarin-Sobrinho,[a] José Carlos Netto-Ferreira[a,d]

[a] Universidade Federal Rural do Rio de Janeiro, Departamento de Química, CEP 23890-000, Seropédica-RJ, Brazil.

[b] Universidade Federal do Rio de Janeiro, Instituto de Química, Ilha do Fundão, CEP 21941-909, Rio de Janeiro-RJ, Brazil.

[c] Universidade Federal Fluminense, Instituto de Química, CEP 24020-141, Niterói-RJ, Brazil.

[d] Instituto Nacional de Metrologia, Qualidade e Tecnologia, Divisão de Metrologia Química, CEP 25250-020, Duque de Caxias-RJ, Brazil.

* romulorcf@yahoo.com.br

Recebido em 4 de janeiro de 2018. Aceito para publicação em 4 de abril de 2018

1. Introduction

Human serum albumin (HSA) is the major soluble extracellular protein of human plasma, being in the concentration of 34-50 gdm^{-3}, which accounts for 60% of the total plasma protein content.[1] From the structural point of view, HSA is a single-chain, non-glycosylated polypeptide with a molecular weight of 66,500 Da and containing 585 amino acids. The approximate three-dimensional shape of HSA resembles a heart shape, with approximate dimensions of 80 ×

80 × 30 Å, which can be described as an ellipsoid (helical protein with turns and extended loops) divided into three domains (I, II, III) and each domain into two subdomain (A and B). The presence of just one tryptophan residue (Trp-214), located in the subdomain IIA, which is also known as Sudlow's site I, is the responsible for its intrinsic fluorescent properties.[2-4] HSA is stable in the pH range of 4-9, can be soluble in 40% ethanol, and can be heated at 60 °C for up to 10 h without deleterious effects.[5] HSA possesses a unique capability to bind, covalently or reversibly, a significant number of various endogenous and exogenous compounds.[6-8] Thus, drug binding influences the distribution, excretion, metabolism, and interaction with the target tissues and an understanding of the features of drug interaction with HSA can provide insights into drug therapy and design.[9] These properties, as well as its preferential uptake in tumor and inflamed tissue, its ready availability, its biodegradability, and its lack of toxicity and immunogenicity, make it an ideal candidate for drug delivery.[5]

Naphthoquinones are an important class of quinones, widely identified as functional metabolites from various plants, microbes, and marine organisms.[10] From the structural point of view, naphthoquinones are naphthalene derivatives bearing two carbonyl oxygen atoms. Even though there are several isoforms of naphthoquinones, the most stable and widely reported one is 1,4-naphthoquinone. Based on this scaffold, a significant class of efficacious analogs has been discovered including simply modified naphthoquinones, i.e. lawsone, shikonin, juglone, plumbagin, menadione (also known as synthetic vitamin K3) and more complicated derivatives such as anthraquinone doxorubicin and naphthoquinone epoxide napabucasin.[11,12] Both synthetic and natural naphthoquinone derivatives show a wide range of pharmacological activities, such as anticancer,[13-15] antibacterial,[16,17] antiviral,[18] antioxidant[19,20] and anti-inflammatory.[21-23] In this sense, two synthetic α-pyran naphthoquinones (2-phenyl-2,3-dihydronaphtho[2,3-b]furan-4,9-dione (**FNP**) and 2-(4-bromophenyl)-2,3-dihydronaphtho[2,3-b]furan-4,9-dione (**FNP4Br**), Figure 1) have shown potential biological activity as inhibitor of *Mycobacterium tuberculosis* strain H37Rv,[24] as well as possible inhibitor of six strains of Candida: *C. albicans, C. krusei, C. parapsilosis, C. kefyr, C. tropicalis and C. dubliniensis*,[25] and inhibitor of four human tumor cell lines: HL-60 (leukemia), SF-295 (CNS), HCT-8 (colon) and MDA-MB435 (melanoma).[26]

Recently, our group has published results on the interaction between serum albumin and α-lapachone - a natural 1,4-naphthoquinone – by spectroscopic and molecular docking methods.[27] In this case, -lapachone may interact spontaneously and strongly with serum albumin through a ground-state association. However, there is no significant disturbance in the albumin secondary structure. There is just one main binding site (Sudlow's site I) for this association, which occurs endothermically and is possibly driven by hydrophobic factors. In this case, hydrogen bonding and hydrophobic interactions are the main binding forces.[27]

To continue the exploration of the binding ability between serum albumin and potential drugs containing the 1,4-naphthoquinone moiety, the present study is aimed to investigate the interaction between HSA:**FNP** and HSA:**FNP4Br**. Circular dichroism spectroscopy was applied to investigate possible perturbation on the secondary structure of the protein upon ligand binding, while steady-state and time-resolved fluorescence spectroscopy were employed to determine binding constant parameters and computational calculations via molecular docking were applied to offer a molecular level explanation on the binding ability.

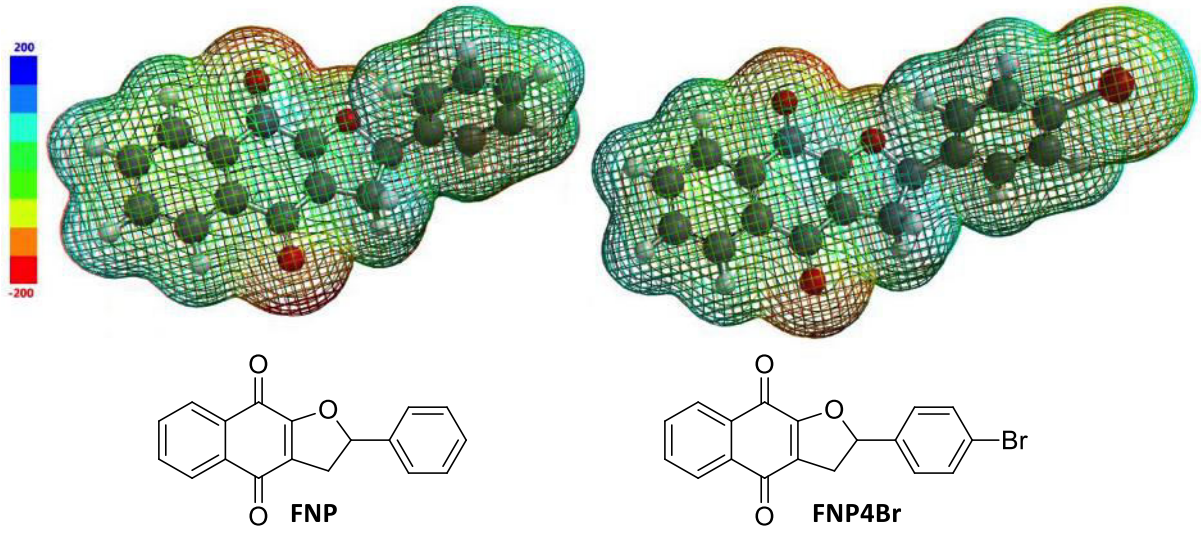

Figure 1. Chemical structure and the theoretical potential electrostatic map for **FNP** and **FNP4Br**

2. Experimental

2.1. Materials

Commercially available HSA and PBS buffer (pH = 7.4) were obtained from Sigma-Aldrich Chemical Company. Water used in all experiments was Millipore grade. Methanol (spectroscopic grade) was obtained from Tedia Ltd. The samples **FNP** and **FNP4Br** were synthesized and characterized according to a previous publication.[25]

2.2. Spectroscopic measurements

UV-Vis and steady-state fluorescence spectra were measured on a Jasco J-815 fluorimeter using a quartz cell (1.00 cm optical path) and employing a thermostatic cuvette holder Jasco PFD-425S15F. The circular dichroism (CD) spectra were measured in a spectropolarimeter Jasco J-815, employing the same thermostatic cuvette holder as described above. All spectra were recorded with appropriate background corrections. Because **FNP** and **FNP4Br** show absorption lower than 0.10 a.u. at 280 and 340 nm (Figure 1S, supplementary material), the correction for the inner filter effect was not necessary.[28]

The UV-Vis absorption spectrum for **FNP** and **FNP4Br** ($2.70x10^{-5}$ M, in PBS) was measured in the 200-450 nm range at 310 K. The steady-state fluorescence measurements were carried out in the 290-450 nm range (λ_{exc} = 280 nm) at 305 K, 310 K and 315 K using 3.0 mL of a HSA solution ($1.00x10^{-5}$ M, in PBS). The addition of **FNP** or **FNP4Br** to the HSA solution was done manually by using a microsyringe, achieving final concentrations of 0.34; 0.67; 1.01; 1.35; 1.69; 2.02; 2.36 and $2.70x10^{-5}$ M.

The CD analysis was carried out using 3.0 mL of a HSA ($1.00x10^{-6}$ M in PBS) solution without and in the presence of **FNP** or **FNP4Br**, in the 200-250 nm range, at 310 K. The HSA:ligand proportion used was 1:0; 1:4; 1:8; 1:16 and 1:32. In this case, the molar concentration of each ligand was 0.40; 0.79; 1.56 and $3.03x10^{-4}$ M. The intensity of the signal from the CD spectra was expressed as mean residue ellipticity (MRE), defined according to equation 1:[29]

$$MRE = \frac{\theta}{(10.n.l.C_P)} \quad (1)$$

where θ, *n*, *l* and C_p are the observed CD (in milli-degrees), number of amino acid residues (585 for HSA),[30] optical pathlength of the cell (1.00 cm) and molar concentration of HSA ($1.00x10^{-6}$ M), respectively.

Time-resolved fluorescence measurements were performed on a model FL920 CD fluorimeter from Edinburgh Instruments, equipped with an EPL laser (λ_{exc} = 280±10 nm; pulse of 850 ps with energy of 1.8 μW/pulse, monitoring emission at 340 nm). The time-resolved fluorescence decay of a 3.0 mL solution of HSA ($1.00x10^{-5}$ M, in PBS) was measured in the absence and presence of **FNP** or **FNP4Br** ($2.70x10^{-5}$ M).

2.3. Theoretical calculations

The structure for **FNP** and **FNP4Br** was built and energy-minimized by Density Functional Theory (DFT) calculations, with B3LYP potential and basis set 6-31G* available in the Spartan'14 program. The crystallographic structure of HSA was obtained from the Protein Data Bank (1N5U).[30] The molecular docking studies were performed with GOLD 5.2 program (CCDC, *Cambridge Crystallographic Data Centre*).

The hydrogen atoms were added to the albumin structure according to the data inferred by GOLD 5.2 program on the ionization and tautomeric states. Docking interaction cavity in the protein was established with a 10 Å radius from the Trp-214 residue. The number of genetic operations (crossover, migration, mutation) in each docking run used in the search procedure was set to 100,000. The scoring function used was '*ChemPLP*', which is the default function of the GOLD 5.2 program.[31] For more details, see previous publications.[32,33]

3. Results and Discussion

3.1. Spectroscopic analysis of the interaction HSA:FNP and HSA:FNP4Br

Steady-state fluorescence quenching measurement is an important method to study the interaction of small molecules with a biomolecule. The steady-state fluorescence measurement can give some information on the binding of small molecules to a protein, such as the main binding mechanism, binding mode, binding constant and number of binding sites.[34] The intrinsic protein fluorescence originates from the aromatic amino acids tryptophan (Trp), tyrosine (Tyr) and phenylalanine (Phe). However, the indole group of Trp residue is the dominant source of UV absorbance and fluorescence emission in the protein. In the present case, when λ_{exc} = 280 nm, the maximum steady-state fluorescence emission at λ_{em} = 340 nm does not present contribution from the Phe. Similarly, the contribution from the Tyr residue is not significant. Therefore, the most contribution for HSA fluorescence is due to Trp residue.[35] Figure 2 depicts the steady-state fluorescence emission of HSA ($1.00x10^{-5}$ M) and its fluorescence quenching upon successive additions of either **FNP** or **FNP4Br**, at pH = 7.4 and 310 K. Since fluorescence quenching can be observed upon ligand addition, this result can indicate that both samples might have been located next to the Trp-214 residue.[32]

It is important to highlight that the fluorescence emission maximum of proteins, including HSA, mainly reflect the average exposure of Trp residue to the aqueous phase and is highly sensitive to the local environment. Thus it is often used as a reporter group for binding ability, as well as protein conformational changes, through spectral shifts.[35] The slight blue shift observed at the wavelength of the maximum emission of HSA upon **FNP** (from 340 to 332 nm) and **FNP4Br** binding (from 340 to 335 nm) is clear evidence of an increase in the

hydrophobicity around the Trp-214 residue, with the presence of these samples being also responsible for perturbations in the albumin structure.[36]

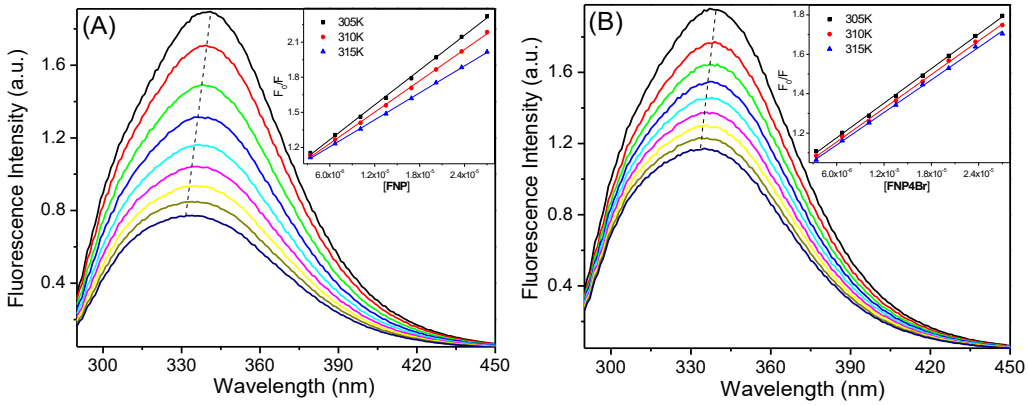

Figure 2. Steady-state fluorescence emission of HSA and its quenching by successive additions of **FNP** (A) and **FNP4Br** (B) at pH = 7.4 and 310 K. *Insets*: Stern-Volmer plot for the interaction HSA:**FNP** (*inset* A) and HSA:**FNP4Br** (*inset* B) at 305 K, 310 K and 315 K. [HSA] = 1.00x10^{-5} M and [**FNP**] = [**FNP4Br**] = 0.34; 0.67; 1.01; 1.35; 1.69; 2.02; 2.36 and 2.70x10^{-5} M

Fluorescence quenching proceeds *via* different mechanisms, which are usually classified as dynamic or static quenching. In some cases, static and dynamic quenching can participate in simultaneously. Dynamic quenching depends upon diffusion effects. Hence, the diffusion coefficient and bimolecular quenching constant would be larger at higher temperatures. On the other hand, static quenching generates a non-fluorescent complex with a consequent decrease of the quenching rate constant value upon increasing the temperature.[37] To obtain information about the main fluorescence quenching mechanism of HSA by **FNP** and **FNP4Br**, a Stern-Volmer analysis (equation 2) was applied:

$$\frac{F_0}{F} = 1 + k_q \tau_0 [Q] = 1 + K_{SV}[Q] \qquad (2)$$

where F_0 and F are the steady state fluorescence intensities of HSA in the absence and presence of each ligand, respectively. [Q], K_{SV} and k_q are the ligand concentration, Stern-Volmer quenching constant and bimolecular quenching rate constant, respectively. τ_0 is the experimental fluorescence lifetime of HSA in the absence of the ligand (5.82±0.12)x10^{-9} s.

The Stern-Volmer plots of F_0/F *versus* [Q] for the fluorescence quenching mechanism of HSA by **FNP** or **FNP4Br** at 305 K, 310 K, and 315 K are showed as an *inset* in Figure 2, and the calculated K_{SV} and k_q values are presented in Table 1. Since the K_{SV} values for HSA:**FNP** and HSA:**FNP4Br** decrease with the increase of temperature and the k_q values are in the order of 10^{12} $M^{-1}s^{-1}$ - higher than the maximum scatter collision rate constant (2.00x10^{10} $M^{-1}s^{-1}$)[38] - a ground-state association can occur between HSA and **FNP** or **FNP4Br**. In other words, the main fluorescence quenching is occurring *via* a static mechanism.[39]

Table 1. Binding constant values (K_{SV}, k_q, n, K_b, $\Delta H°$, $\Delta S°$ and $\Delta G°$) for the interaction between HSA:**FNP** and HSA:**FNP4Br** at 305 K, 310 K and 315 K

Code	T (K)	K_{SV} (x10^4) (M^{-1})	k_q (x10^{12}) ($M^{-1}s^{-1}$)	n	K_b (x10^5) (M^{-1})	$\Delta H°$ (kJmol^{-1})	$\Delta S°$ (kJmol^{-1}K^{-1})	$\Delta G°$ (kJmol^{-1})
	305	4.96±0.06	8.52	1.07±0.04	8.40±0.26			-28.8
FNP	310	4.47±0.05	7.68	1.06±0.02	7.54±0.26	-15.1±0.29	0.045±0.004	-29.1
	315	3.84±0.03	6.60	1.04±0.01	6.96±0.26			-29.3
	305	2.92±0.03	5.02	0.96±0.07	1.69±0.07			-24.6
FNP4Br	310	2.85±0.04	4.89	0.95±0.06	1.64±0.09	-3.52±0.29	0.069±0.001	-24.9
	315	2.75±0.04	4.73	0.95±0.09	1.61±0.06			-25.3

Obs: r^2 for K_{SV} and k_q: 0.9985-0.9997; r^2 for n and K_b: 0.9976-0.9999; r^2 for $\Delta H°$, $\Delta S°$ and $\Delta G°$: 0.9870-0.9883.

In order to further confirm the static mechanism as the main fluorescence quenching process for the interaction HSA:**FNP** and HSA:**FNP4Br**, time-resolved fluorescence measurements were carried out for HSA without and in the presence of each ligand under study at pH 7.4. Figure 3 and Table 2 depict time-resolved fluorescence decays and their parameters for HSA emission without and in the presence of the 1,4-naphthoquinone derivatives. Free HSA showed two fluorescence lifetimes (τ_1=1.76±0.14 ns, 23.9% contribution and τ_2=5.82±0.12 ns,, 76.1% contribution), which is in full agreement with literature results.[40] Addition of **FNP** or **FNP4Br** did not change significantly the albumin lifetime, *i.e.* τ_2 decreases from 5.82±0.12 ns for pure HSA to 5.79±0.10 and 5.75±0.10 ns for HSA:**FNP** and HSA:**FNP4Br**, respectively, with these values being inside the experimental error. Thus, a ground-state association is occurring for both samples, *i. e* a static mechanism.[33]

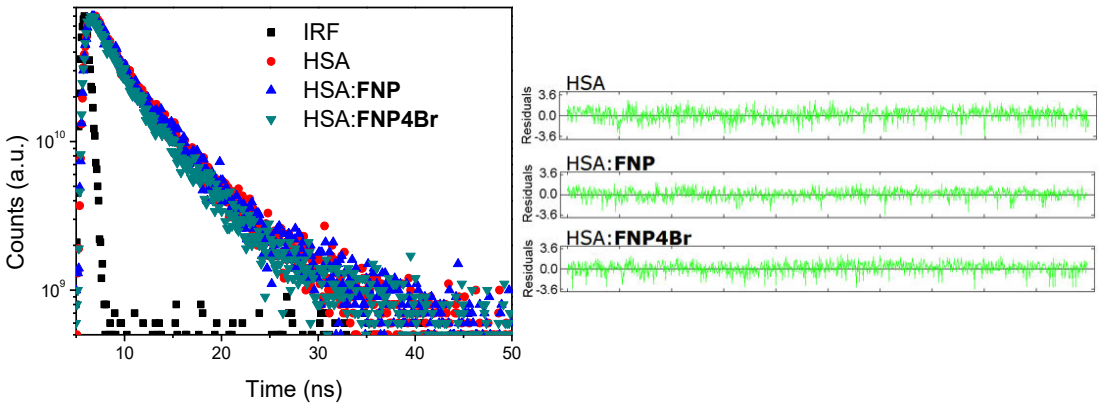

Figure 3. Time-resolved fluorescence decays and its residuals for HSA without and in the presence of **FNP** or **FNP4Br** at pH = 7.4 and room temperature. [HSA] = 1.00x10^{-5} M and [**FNP**] = [**FNP4Br**] = 2.70x10^{-5} M

Table 2. Time-resolved fluorescence parameters for HSA without and in the presence of **FNP** or **FNP4Br** at pH = 7.4 and room temperature

Code	τ_1 (ns)	Relative %	τ_2 (ns)	Relative %	χ^2
HSA	1.76±0.14	23.9	5.82±0.12	76.1	1.061
HSA:**FNP**	1.71±0.10	29.5	5.79±0.10	70.5	1.050
HSA:**FNP4Br**	1.69±0.10	27.8	5.75±0.11	72.2	1.044

The evaluation of the binding constant (K_b) between serum albumin and a ligand is important to understand its distribution in the plasma, body tissues and organs.[41] When small molecules bind independently to a set of equivalent sites on a macromolecule, the equilibrium between free and bound molecules is given by the equation 3 and Figure 4:[42]

$$\log\left(\frac{F_0 - F}{F}\right) = \log K_b + n \log[Q] \quad (3)$$

where F_0 and F are the steady state fluorescence intensities of HSA in the absence and presence each ligand, respectively. K_b and n are the binding constant and the number of binding sites, respectively.

The calculated number of binding sites is approximately 1.00 (Table 1), indicating the existence of just one main binding site in the serum albumin structure for both ligands.[43] The K_b values for the interaction HSA:**FNP** and HSA:**FNP4Br** are in the order of 10^4 M^{-1}, indicating that the 1,4-naphthoquinone derivatives under study can interact moderately with serum albumin.[44,45] In addition, the decrease in the K_b values with the increase of temperature suggests the lesser stability of HSA:1,4-naphthoquinone derivatives complex at higher temperature, being in full accordance with the existence of a static fluorescence quenching mechanism as described above.[46] By comparing the binding constant values with that of the interaction serum albumin and α-lapachone – a natural 1,4-naphthoquinone – the derivatives under study, *i. e* **FNP** and **FNP4Br**, showed better binding ability than α-lapachone.[27]

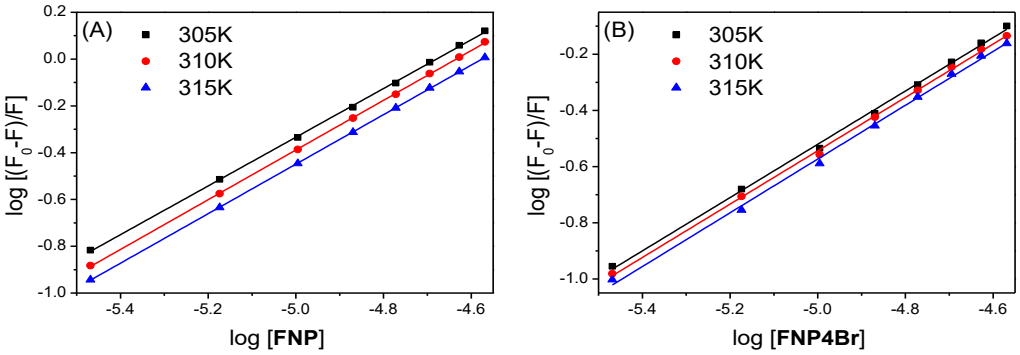

Figure 4. Double logarithmic plot for the interaction HSA:**FNP** (A) and HSA:**FNP4Br** (B) at pH = 7.4, at 305 K, 310 K and 315 K. [HSA] = 1.00x10^{-5} M and [**FNP**] = [**FNP4Br**] = 0.34; 0.67; 1.01; 1.35; 1.69; 2.02; 2.36 and 2.70x10^{-5} M

Essentially, there are four types of non-covalent interactions when a ligand binds to a protein, *i. e* hydrogen bond, van der Waals forces, lipophilic and electrostatic interactions. The thermodynamic parameters of binding ($\Delta H°$ and $\Delta S°$) are used as an evidence in identifying the nature of the acting forces.[44] The thermodynamic parameters associated with the interaction between HSA with **FNP** and **FNP4Br** were calculated according to the van't Hoff (Figure 2S, supplementary material) and Gibb's free energy equations – equations 4A and 4B:[47]

$$\ln K_a = -\frac{\Delta H^0}{RT} + \frac{\Delta S^0}{R} \quad (4A)$$

$$\Delta G^0 = \Delta H^0 - T\Delta S^0 \quad (4B)$$

where $\Delta H°$, $\Delta S°$ and $\Delta G°$ are the enthalpy, entropy and Gibbs' free energy change, respectively. T and R are the temperature (305 K, 310 K and 315 K) and gas constant (8.3145 Jmol^{-1}K^{-1}), respectively.

The values of thermodynamic parameters are presented in Table 1, with $\Delta G° < 0$ indicating that the binding process for HSA:**FNP** and HSA:**FNP4Br** is spontaneous. The negative and positive values of enthalpy and entropy change, respectively, suggest that the binding is enthalpy and entropy driven.[48] Also, the binding involves an exothermic association as manifested by the negative $\Delta H°$ values, which is consistent with the decrease in K_b values with the increase of temperature.[47]

According to Ross and Subramanian's proposal,[49] $\Delta H° < 0$ and $\Delta S° > 0$ are characteristic of hydrogen bonding and electrostatic forces as responsible for the binding process. The **FNP** and **FNP4Br** structures do not show groups capable of ionization at pH = 7.4. Therefore, electrostatic forces ion-ion must not be operating in this association; however, weak electrostatic forces such as dipole-dipole could be occurring, because both ligands presented dipole moment different of zero (theoretical dipole moment 2.14 and 0.78 D, for **FNP** and **FNP4Br**, respectively – Figure 1).[50] From the standpoint of water structure, positive entropy is often regarded as a typical signature of a hydrophobic effect, since the water molecules which are arranged in an

orderly fashion around the ligand and the protein molecule acquire a more random configuration as a result of the hydrophobic effect.[51] Furthermore, the interaction HSA:**FNP4Br** showed higher $\Delta S°$ value than HSA:**FNP**, probably due the fact that the presence of the bromine atom in the 1,4-naphthoquinone derivative structure has increased the solubility of the ligand, causing the presence of more water molecules around the free ligand (see theoretical dipole moment above). Thus, hydrogen bonding and electrostatic interactions are probably the main binding forces responsible for the association HSA:**FNP** and HSA:**FNP4Br**. Additionally, a hydrophobic effect also contributed for this association.

3.2. Perturbation on the secondary structure of HSA upon ligand binding

Circular dichroism (CD) is a sensitive technique to monitor conformational changes in a protein.[46] For this, the CD spectra of HSA in the absence and presence of different concentrations of **FNP** or **FNP4Br** in the proportion HSA:ligand of 1:0; 1:4; 1:8; 1:16 and 1:32 (which results in a concentration of each ligand in the 0.40 - 3.03x10^{-4} M range), were measured at pH = 7.4 and 310 K (Figure 5). The CD spectrum of serum albumin exhibits two negative signals at 208 (π–π* transition) and 222 nm (*n*–π* transition), which are due to the presence of the amide groups forming the peptide bonds.[47]

The α-helix contents of free and combined HSA were calculated from the mean residue ellipticity (MRE) values at 208 and 222 nm using the equations 5A and 5B:[52]

$$\alpha\text{-}helix\% = \frac{\left(-MRE_{208} - 4000\right)}{(33000 - 4000)} \; x\; 100 \qquad (5A)$$

$$\alpha\text{-}helix\,\% = \frac{\left(-MRE_{222} - 2340\right)}{30300} \; x\; 100 \qquad (5B)$$

The CD signal from HSA decreases with the addition of **FNP** or **FNP4Br** (Figure 5), indicating changes in the protein structure upon ligand binding.[53] In addition, the quantitative α-helical % content for HSA without and in the presence of **FNP** or **FNP4Br** changed moderately, mainly in a high concentration of ligand (Table 3), *i. e* 6.60% for HSA:**FNP** and 13.8% HSA:**FNP4Br**, at 208 nm, both ligands in a molar concentration of 3.03x10^{-4} M - proportion 1:32. These results are a clear indication that **FNP** or **FNP4Br** bind in the main polypeptide chain of protein and can destroy the hydrogen bonding networks of the albumin, mainly the bromine derivative.[54]

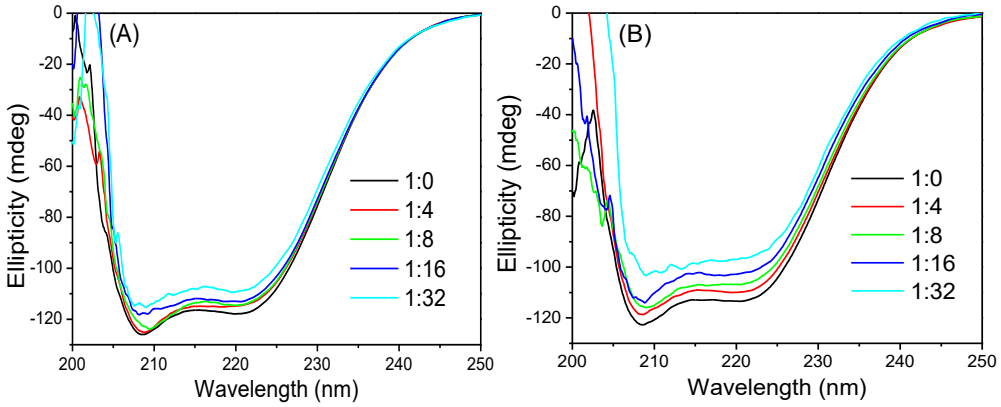

Figure 5. CD spectra for HSA without and in the presence of **FNP** (A) and **FNP4Br** (B), at pH = 7.4 and 310 K, in the proportion HSA:ligand 1:0; 1:4; 1:8; 1:16 and 1:32

Table 3. The α-helical % content for HSA without and in the presence of **FNP** or **FNP4Br** at pH = 7.4 and 310 K

Code	Proportion / HSA:ligand	α-helix % at 208 nm	α-helix % at 222 nm
HSA:**FNP**	1:0	60.1	58.1
	1:4	59.3	56.3
	1:8	57.4	56.0
	1:16	55.8	55.3
	1:32	53.5	53.0
HSA:**FNP4Br**	1:0	58.1	55.6
	1:4	55.9	53.7
	1:8	53.7	51.9
	1:16	52.5	49.6
	1:32	44.3	46.3

3.3. Molecular docking analysis of the interaction HSA:FNP and HSA:FNP4Br

Structurally, HSA consists of three homologous domains (I, II, and III) and each domain comprised the subdomains A and B. The subdomains IIA and IIIA present high affinity for binding different kinds of ligands and are referred as Sudlow's site I and II, respectively.[55] From the spectroscopic results described above – ground-state association and fluorescence quenching - it is known that **FNP** and **FNP4Br** are able to bind near the Trp-214 residue, which is located in subdomain IIA (Sudlow's site I). Thus, in order to offer a molecular level explanation on the binding ability of **FNP** and **FNP4Br** toward HSA, molecular docking calculations were performed.

Figure 6 shows the molecular docking results for the interaction between HSA and **FNP** or **FNP4Br** inside Sudlow's site I. For the association HSA:**FNP**, the oxygen atom from the two carbonyl groups of the ligand structure are acceptors for hydrogen bonding with Trp-214 and Ser-453 residues, within a distance of 1.80 and 3.20 Å, respectively.

Electrostatic interaction *via* dipole-dipole can also occur between the aromatic rings of the ligand structure with Leu-197, Val-343, Leu-456, and Leu-480 residues, within a distance of 3.40; 3.20; 1.95 and 3.00 Å, respectively.

On the other hand, for the association HSA:**FNP4Br**, the oxygen atom of the two carbonyl groups of the ligand structure are acceptors for hydrogen bonding with Lys-194 and Trp-214 residues, within a distance of 2.90 and 1.80 Å, respectively. Electrostatic interaction *via* dipole-dipole can also occur between the aromatic rings of the ligand with Leu-197, Val-342, Pro-446, and Leu-480 residues, within distance a of 2.10; 1.90; 2.50 and 2.60 Å, respectively. Note that even the two ligands having a similar structure, the molecular docking results suggested that the presence of the bromine atom in the **FNP4Br** structure can cause modifications in the type of amino acid residues that participate in the association HSA:1,4-naphthoquinone derivatives, which can reflect in some differences in the binding parameters detected experimentally. Overall, these theoretical results for the interaction HSA:**FNP** and HSA:**FNP4Br** are in full accordance with the intermolecular interactions suggested by the experimental thermodynamic parameters described above.

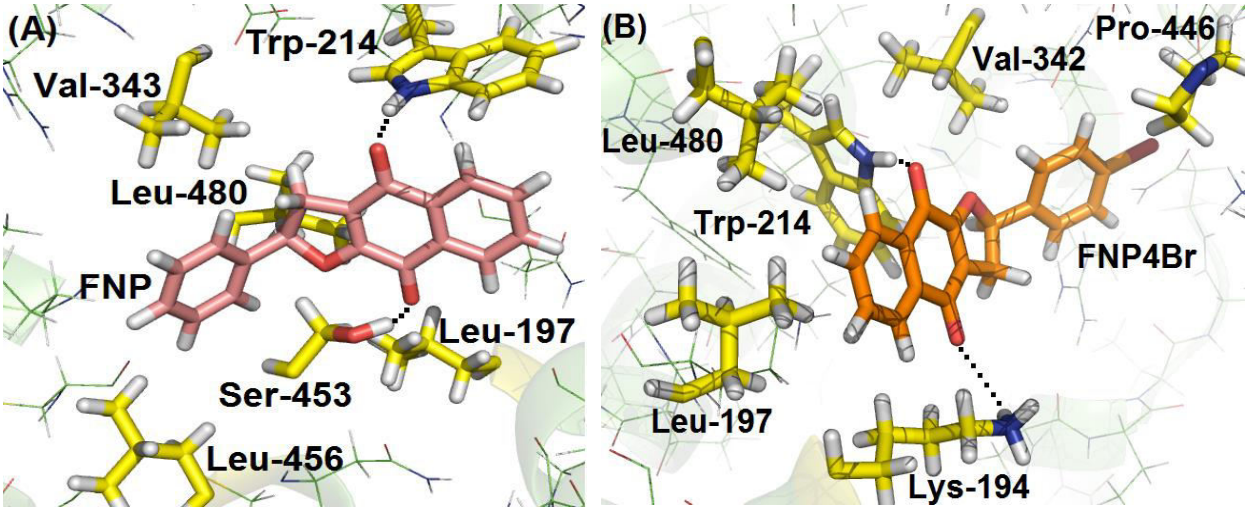

Figure 6. Best score pose for HSA:**FNP** and HSA:**FNP4Br** in Sudlow's site I (*ChemPLP* function). Selected amino acids residues, **FNP** and **FNP4Br** are represented in yellow, beige and orange, respectively. Black dots represent the interaction *via* hydrogen bonding. Hydrogen: white; oxygen: red; nitrogen: dark blue and bromine: carmine

4. Conclusion

The HSA fluorescence quenching upon successive additions of **FNP** and **FNP4Br** follows a static mechanism; therefore, there is a ground-state association HSA:**FNP** and HSA:**FNP4Br**. The interaction between HSA and both ligands is spontaneous, moderate, as well as entropy and enthalpy driven. The binding can change moderately the secondary structure of the albumin, mainly in the presence of **FNP4Br**. Hydrogen bonding and electrostatic interactions (dipole-dipole) are the main binding forces involved in the interaction between HSA and **FNP** or **FNP4Br**. Inside Sudlow's site I, in subdomain IIA, molecular docking results suggest that **FNP** can interact *via* hydrogen bonding and dipole-dipole with Leu-197, Trp-214, Val-343, Ser-453, Leu-456, and Leu-480 residues, while **FNP4Br** can also interact *via* hydrogen bonding and dipole-dipole with Lys-194, Leu-197, Trp-214, Val-342, Pro-446, and Leu-480

residues. Overall, the synthetic molecules **FNP** and **FNP4Br** depict better binding ability than the natural product α-lapachone.

Acknowledgements

This research was supported by the Brazilian funding agencies: Coordenação de Aperfeiçoamento de Pessoal de Nível Superior (CAPES), Conselho Nacional de Desenvolvimento Científico e Tecnológico (CNPq) and Fundação de Amparo à Pesquisa do Estado do Rio de Janeiro (FAPERJ). The authors also acknowledge Prof. Dr. Nanci Camara de Lucas Garden (Chemistry Institute - UFRJ) for the time-resolved fluorescence facilities.

References

[1] Keswani, N.; Choudhary, S.; Kishore, N. Interaction of weakly bound antibiotics neomycin and lincomycin with bovine and human serum albumin: biophysical approach. *The Journal of Biochemistry* **2010**, *148*, 71. [CrossRef] [PubMed]

[2] Yang, F.; Zhang, Y.; Liang, H. Interactive association of drugs binding to human serum albumin. *International Journal of Molecular Science* **2014**, *15*, 3580. [CrossRef] [PubMed]

[3] Fasano, M.; Curry, S.; Terreno, E.; Galliano, M.; Fanali, G.; Narciso, P.; Notari, S.; Ascenzi, P. The extraordinary ligand binding properties of human serum albumin. *IUBMB Life* **2005**, *57*, 787. [CrossRef] [PubMed]

[4] Naveenraj, S.; Anandan, S. Binding of serum albumins with bioactive substances – Nanoparticles to drugs. *Journal of Photochemistry and Photobiology C: Photochemistry Reviews* **2013**, *14,* 53. [CrossRef]

[5] Kratz, F. Albumin as a drug carrier: Design of prodrugs, drug conjugates and nanoparticles. *Journal of Controlled Release* **2008**, *132*, 171. [CrossRef] [PubMed]

[6] Liu, X.; Liang, A.; Shen, Z.; Liu, X.; Zhang, Y.; Dai, Z.; Xiong, B.; Lin, B. Studying drug-plasma protein interactions by two-injector microchip electrophoresis frontal analysis. *Electrophoresis* **2006**, *24*, 5128. [CrossRef] [PubMed]

[7] Basken, N. E.; Mathias, C. J. Elucidation of the human serum albumin (HSA) binding site for the Cu-PTSM and Cu-ATSM radiopharmaceuticals. *Journal of Pharmaceutical Sciences* **2009**, *98*, 2170 [CrossRef] [PubMed]

[8] Zhivkova, Z. D. Studies on drug-human serum albumin binding: the current state of the matter. *Current Pharmaceutical Design* **2015**, *21*, 1817. [CrossRef] [PubMed]

[9] He, L.; Wang, X.; Liu, B.; Wang, J.; Sun, Y.; Gao, E.; Xu, S. Study on the interaction between promethazine hydrochloride and bovine serum albumin by fluorescence spectroscopy. *Journal of Luminescence* **2011**, *131*, 285. [CrossRef] [PubMed]

[10] Babula, P.; Adam, V.; Havel, L.; Kizek, R. Noteworthy secondary metabolites naphthoquinones-their occurrence, pharmacological properties and analysis. *Current Pharmaceutical Analysis* **2009**, *5*, 47. [CrossRef]

[11] Qiu, H.-Y.; Wang, P.-F.; Lin, H.-Y.; Tang, C.-Y.; Zhu, H.-L.; Yang, Y.-H. Naphthoquinones: A continuing source for discovery of therapeutic antineoplastic agents. *Chemical Biology & Drug Design* **2018**, *91*, 681. [CrossRef] [PubMed]

[12] Luft, F. C. Doxorubicin toxicity in the iron age. *Journal of Molecular Medicine* **2006**, *84*, 529 [CrossRef] [PubMed]

[13] da Silva, E. N. Jr.; Souza, M. C. B. V.; Pinto, A. V.; Pinto, M. C. F. R.; Goulart, M O. F.; Barros, F. W. A.; Pessoa, C.; Costa-Lotufo, L. V.; Montenegro, R. C.; de Moraes, M. O.; Ferreira, V. F. Synthesis and potent antitumor activity of new arylamino derivatives of nor-β-lapachone and nor-α-lapachone. *Bioorganic & Medicinal Chemistry* **2007**, *15*, 7035. [CrossRef] [PubMed]

[14] Prachayasittikul, V.; Pingaew, R.; Worachartcheewan, A.; Nantasenamat, C.; Prachayasittikul, S.; Ruchirawat, S.; Prachayasittikul, V. Synthesis, anticancer activity and QSAR study of 1,4-naphthoquinone derivatives. *European*

Journal of Medicinal Chemistry **2014**, *84*, 247. [CrossRef] [PubMed]

[15] Delarmelina, M.; Daltoé, R. D.; Cerri, M. F.; Madeira, K. P.; Rangel, L. B. A.; Júnior, V. L.; Romão, W.; Taranto, A. G.; Greco, S. J. Synthesis, antitumor activity and docking of 2,3-(substituted)-1,4-naphthoquinone derivatives containing nitrogen, oxygen and sulfur. *Journal of the Brazilian Chemical Society* **2015**, *26*, 1804. [CrossRef]

[16] Sánchez-Calvo, J. M.; Barbero, G. R.; Guerrero-Vásquez, G.; Durán, A. G.; Macías, M.; Rodríguez-Iglesias, M. A.; Molinillo, J. M. G.; Macías, F. A. Synthesis, antibacterial and antifungal activities of naphthoquinone derivatives: a structure–activity relationship study. *Medicinal Chemistry Research* **2016**, *25*, 1274. [CrossRef] [PubMed]

[17] Janeczko, M.; Demchuk, O. M.; Strzelecka, D.; Kubiński, K.; Masłyk, M. New family of antimicrobial agents derived from 1,4-naphthoquinone. *European Journal of Medicinal Chemistry* **2016**, *124*, 1019. [CrossRef] [PubMed]

[18] Tandon, V. K.; Yadav, D. B.; Singh, R. V.; Chatuverdi, A. K.; Shukla, P. K. Synthesis and biological evaluation of novel 1,4-naphthoquinone derivatives as antibacterial and antiviral agents. *Bioorganic & Medicinal Chemistry Letters* **2005**, *15*, 5324. [CrossRef] [PubMed]

[19] de Oliveira, A. S.; Brighente, I. M. C.; Lund, R. G.; Llanes, L. C.; Nunes, R. J.; Bretanha, L. C.; Yunes, R. A.; Carvalho, P. H. A.; Ribeiro, J. S. Antioxidant and antifungal activity of naphthoquinones dimeric derived from lawsone. *Journal of Biosciences and Medicines* **2017**, *5*, 39. [CrossRef]

[20] Deniz, N. G.; Ibis, C.; Gokmen, Z.; Stasevych, M.; Novikov, V.; Komarovska-Porokhnyavets, O.; Ozyurek, M.; Guclu, K.; Karakas, D.; Ulukaya, E. Design, synthesis, biological evaluation, and antioxidant and cytotoxic activity of heteroatom-substituted 1,4-naphtho- and benzoquinones. *Chemical and Pharmaceutical Bulletin* **2015**, *63*, 1029. [CrossRef] [PubMed]

[21] Nicolaides, D. N.; Gautam, D. R.; Litinas, K. E.; Litina, D. J. H.; Fylaktakidou, K. C. Synthesis and evaluation of the antioxidant and anti-inflammatory activities of some benzo[l]khellactone derivatives and analogues. *European Journal of Medicinal Chemistry* **2004**, *39*, 323. [CrossRef] [PubMed]

[22] Soares, A. S.; Barbosa, F. L.; Rüdiger, A. L.; Hughes, D. L.; Salvador, M. J.; Zampronio, A. R.; Stefanello, M. É. A. Naphthoquinones of *Sinningia reitzii* and anti-inflammatory/antinociceptive activities of 8-hydroxydehydrodunnione. *Journal of Natural Products* **2017**, *80*, 1837. [CrossRef] [PubMed]

[23] Dong, M.; Liu, D.; Li, Y. H.; Chen, X. Q.; Luo, K.; Zhang, Y. M.; Li, R. T. Naphthoquinones from Onosma paniculatum with potential anti-inflammatory activity. *Planta Medica* **2017**, *83*, 631. [CrossRef] [PubMed]

[24] Ferreira, S. B.; da Silva, F. C.; Bezerra, F. A. F. M.; Lourenço, M. C. S.; Kaiser, C. R.; Pinto, A. C.; Ferreira, V. F. Synthesis of α- and β-Pyran Naphthoquinones as a New Class of Antitubercular Agents. *Archiv der Pharmazie* **2010**, *343*, 81. [CrossRef] [PubMed]

[25] Freire, C. P. V.; Ferreira, S. B.; de Oliveira, N. S. M.; Matsuura, A. B. J.; Gama, I. L.; da Silva, F. C.; de Souza, M. C. B. V.; Lima, E. S.; Ferreira, V. F. Synthesis and biological evaluation of substituted α- and β-2,3-dihydrofuran naphthoquinones as potent anticandidal agents. *Medicinal Chemistry Communications* **2010**, *1*, 229. [CrossRef]

[26] Ferreira, F. R.; Ferreira, S. B.; Araújo, A. J.; Filho, J. D. B. M.; Pessoa, C.; Moraes, M. O.; Costa-Lotufo, L. V.; Montenegro, R. C.; da Silva, F. C.; Ferreira, V. F.; da Costa, J. G.; de Abreu, F. C.; Goulart, M. O. F. Arylated α- and β-dihydrofuran naphthoquinones: Electrochemical parameters, evaluation of antitumor activity and their correlation. *Electrochimica Acta* **2013**, *110*, 634. [CrossRef]

[27] Chaves, O. A.; Schaeffer, E.; Sant'Anna, C. M. R.; Netto-Ferreira, J. C.; Cesarin-Sobrinho, D.; Ferreira, A. B. B. Insight into the interaction between α-lapachone and bovine serum albumin employing a spectroscopic and computational approach. *Mediterranean Journal of Chemistry* **2016**, *5*, 331. [CrossRef]

[28] Chaves, O. A.; Jesus, C. S. H.; Cruz, P. F.; Sant'Anna, C. M. R.; Brito, R. M. M.; Serpa, C. Evaluation by fluorescence, STD-NMR, docking and semi-empirical calculations of the *o*-NBA photo-acid interaction with BSA. *Spectrochimica Acta Part A: Molecular and Biomolecular Spectroscopy* **2016**, *169*, 175. [CrossRef] [PubMed]

[29] Chaves, O. A.; Mathew, B.; Cesarin-Sobrinho, D.; Lakshminarayanan, B.; Joy, M.; Mathew, G. E.; Suresh, J.; Netto-Ferreira, J. C. Spectroscopic, zeta potential and molecular docking analysis on the interaction between human serum albumin and halogenated thienyl chalcones. *Journal of Molecular Liquids* **2017**, *242*, 1018. [CrossRef]

[30] Wardell, M.; Wang, Z.; Ho, J. X.; Robert, J.; Ruker, F.; Ruble, J.; Carter, D. C. The atomic structure of human methemalbumin at 1.9 A. *Biochemical and Biophysical Research Communications* **2002**, *291,* 913. [CrossRef] [PubMed]

[31] The Cambridge Crystallographic Data Centre (CCDC) website <http://www.ccdc.cam.ac.uk/solutions/csd-discovery/components/gold/>. Access in: 26 december 2017.

[32] Chaves, O. A.; Amorim, A. P. O.; Castro, L. H. E.; Sant'Anna, C. M. R.; de Oliveira, M. C. C.; Cesarin-Sobrinho, D.; Netto-Ferreira, J. C.; Ferreira, A. B. B. Fluorescence and Docking Studies of the Interaction between Human Serum Albumin and Pheophytin. *Molecules* **2015**, *20*, 19526. [CrossRef] [PubMed]

[33] Chaves, O. A.; de Oliveira, C. H. C. S.; Ferreira, R. C.; Pereira, R. P.; de Melos, J. L. R.; Rodrigues-Santos, C. E.; Echevarria, A.; Cesarin-Sobrinho, D. Investigation of interaction between human plasmatic albumin and potential fluorinated anti-trypanosomal drugs. *Journal of Fluorine Chemistry* **2017**, *199*, 103. [CrossRef]

[34] Sun, Y.; Zhang, H.; Sun, Y.; Zhang, Y.; Liu, H.; Cheng, J.; Bi, S.; Zhang, H. Study of interaction between protein and main active components in *Citrus aurantium* L. by optical spectroscopy. *Journal of Luminescence* **2010**, *130*, 270. [CrossRef]

[35] Lakowicz, J. R.; *Principles of Fluorescence Spectroscopy*, 3rd. ed., Springer: New York, 2006.

[36] Molina-Bolívar, J. A.; Ruiz, C. C.; Galisteo-González, F.; Donnell, M. M. -O.´; Parra, A. Simultaneous presence of dynamic and sphere action component in the fluorescence quenching of human serum albumin by diphthaloylmaslinic acid. *Journal of Luminescence* **2016**, *178*, 259. [CrossRef]

[37] Sun, Y.; Wei, S.; Yin, C.; Liu, L.; Hu, C.; Zhao, Y.; Ye, Y.; Hu, X.; Fan, J. Synthesis and spectroscopic characterization of 4-butoxyethoxy-N-octadecyl-1,8-naphthalimide as a new fluorescent probe for the determination of proteins. *Bioorganic & Medicinal Chemistry Letters* **2011**, *21*, 3798. [CrossRef] [PubMed]

[38] Peng, X.; Yu, J.; Yu, Q.; Bian, H.; Huang, F.; Liang, H. Binding of Engeletin with Bovine Serum Albumin: Insights from Spectroscopic Investigations. *Journal of Fluorescence* **2012**, *22*, 511. [CrossRef]

[39] Guo, X.J.; Zhang, L.; Sun, X.D.; Han, X.W.; Guo, C.; Kang, P. L. Spectroscopic studies on the interaction between sodium ozagrel and bovine serum albumin. *Journal of Molecular Structure* **2009**, *928*, 114. [CrossRef]

[40] Sun, H.; Liu, Y.; Li, M.; Han, S.; Yang, X.; Liu, R. Toxic effects of chrysoidine on human serum albumin: isothermal titration calorimetry and spectroscopic investigations. *Luminescence* **2016**, *31*, 335. [CrossRef] [PubMed]

[41] Chaves, O. A.; Jesus, C. S. H.; Henriques, E. S.; Brito, R. M. M.; Serpa, C. *In situ* ultra-fast heat deposition does not perturb the structure of serum albumin. *Photochemistry & Photobiology Science* **2016**, *15*, 1524. [CrossRef] [PubMed]

[42] Guo, X.; Han, X.; Tong, J.; Guo, C.; Yang, W.; Zhu, J.; Fu, B. The investigation of the interaction between piracetam and bovine serum albumin by spectroscopic methods. *Journal of Molecular Structure* **2010**, *966*, 129. [CrossRef]

[43] Naveenraj, S.; Raj, M. R.; Anandan, S. Binding interaction between serum albumins and perylene-3,4,9,10-tetracarboxylate e A spectroscopic investigation. *Dyes and Pigments* **2012**, *94*, 330. [CrossRef]

[44] Chaves, O. A.; da Silva, V. A.; Sant'Anna, C. M. R.; Ferreira, A. B. B.; Ribeiro, T. A. N.; de Carvalho, M. G.; Cesarin-Sobrinho, D.; Netto-

Ferreira, J. C. Binding studies of lophirone B with bovine serum albumin (BSA): Combination of spectroscopic and molecular docking techniques. *Journal of Molecular Structure* **2017**, *1128*, 606. [CrossRef]

[45] Chaves, O. A.; Cesarin-Sobrinho, D.; Sant'Anna, C. M. R.; de Carvalho, M. G.; Suzart, L. R.; Catunda-Junior, F. E. A.; Netto-Ferreira, J. C.; Ferreira, A. B. B. Probing the interaction between 7-O-β-D-glucopyranosyl-6-(3-methylbut-2-enyl)-5,40-dihydroxyflavonol with bovine serum albumin (BSA). *Journal of Photochemistry and Photobiology A: Chemistry* **2017**, *336*, 32. [CrossRef]

[46] Katrahalli, U.; Kalalbandi, V. K. A.; Jaldappagari, S. The effect of anti-tubercular drug, ethionamide on the secondary structure of serum albumins: A biophysical study. *Journal of Pharmaceutical and Biomedical Analysis* **2012**, *59*, 102. [CrossRef] [PubMed]

[47] Chaves, O. A.; Teixeira, F. S. M.; Guimarães, H. A.; Braz-Filho, R.; Vieira, I. J. C.; Sant'Anna, C. M. R.; Netto-Ferreira, J. C.; Cesarin-Sobrinho, D.; Ferreira, A. B. B. Studies of the Interaction between BSA and a Plumeran Indole Alkaloid Isolated from the Stem Bark of *Aspidosperma cylindrocarpon* (Apocynaceae). *Journal of the Brazilian Chemical Society* **2017**, *28*, 1229 [CrossRef]

[48] Zhang, Z.; Tang, R. Synthesis and fluorescence properties of Tb(III) complex with a novel β-diketone ligand as well as spectroscopic studies on the interaction between Tb(III) complex and bovine serum albumin. *Journal of Molecular Structure* **2012**, *1010*, 116. [CrossRef]

[49] Ross, P. D.; Subramanian, S. Thermodynamics of protein association reactions: Forces contributing to stability. *Biochemistry* **1981**, *20*, 3096. [CrossRef] [PubMed]

[50] Jiang, H.; Chen, R.; Pu, H. Study on the interaction between tabersonine and human serum albumin by optical spectroscopy and molecular modeling methods. *Journal of Luminescence* **2012**, *132*, 592. [CrossRef]

[51] Bi, S.; Yan, L.; Pang, B.; Wang, Y. Investigation of three flavonoids binding to bovine serum albumin using molecular fluorescence technique. *Journal of Luminescence* **2012**, *132*, 132. [CrossRef] [PubMed]

[52] Hu, Y.-J.; Yue, H.-L.; Li, X.-L.; Zhang, S.-S.; Tang, E.; Zhang, L.-P. Molecular spectroscopic studies on the interaction of morin with bovine serum albumin. *Journal of Photochemistry and Photobiology B: Biology* **2012**, *112*, 16. [CrossRef] [PubMed]

[53] Du, W.; Teng, T.; Zhou, C.-C.; Xi, L.; Wang, J.-Z. Spectroscopic studies on the interaction of bovine serum albumin with ginkgolic acid: Binding characteristics and structural analysis. *Journal of Luminescence* **2012**, *132*, 1207. [CrossRef]

[54] Hussein, B. H. M. Spectroscopic studies of 7,8-dihydroxy-4-methyl coumarin and its interaction with bovine serum albumin. *Journal of Luminescence* **2011**, *131*, 900. [CrossRef]

[55] Chibber, S.; Ahmad, I. Molecular docking, a tool to determine interaction of CuO and TiO_2 nanoparticles with human serum albumin. *Biochemistry and Biophysics Reports* **2016**, *6*, 63. [CrossRef] [PubMed]